Brachial artery vasodilatory response and wall shear rate determined by multi-gate Doppler in a healthy young cohort

Authors:

Kunihiko Aizawa,[1] Sara Sbragi,[2] Alessandro Ramalli,[3] Piero Tortoli,[3] Francesco Casanova,[1] Carmela Morizzo,[2] Clare E Thorn,[1] Angela C Shore,[1] Phillip E Gates,[1] Carlo Palombo.[2]

Affiliations:

[1] Diabetes and Vascular Medicine Research Centre, NIHR Exeter Clinical Research Facility, University of Exeter Medical School, Exeter, UK

[2] Department of Surgical, Medical, Molecular Pathology and Critical Care Medicine, University of Pisa, Pisa, Italy

[3] Department of Information Engineering, University of Florence, Florence, Italy

Running Head:

Brachial vasodilation and wall shear rate in the young

Author Contributions

Conception and design of research: KA, PT, AS, PG, CP. Performed experiments: KA, SS, FC, CM, CT, PG. Analyzed data: KA, AR, PG. Interpreted results of experiments: KA, PT, AS, PG, CP. Prepared figures: KA, AR. Drafted manuscript: KA, AR, PG. Edited and revised manuscript: KA, SS, AR, PT, FC, CM, CT, AS, PG, CP. Approved final version of manuscript: KA, SS, AR, PT, FC, CM, CT, AS, PG, CP.

Corresponding Author:

Kunihiko Aizawa, PhD
Diabetes and Vascular Medicine Research Centre
University of Exeter Medical School
NIHR Exeter Clinical Research Facility
Barrack Road, Exeter
EX2 5AX, UK
+44 1392 403081 (TEL)
+44 1392 403027 (FAX)
k.aizawa@exeter.ac.uk

ABSTRACT:

Wall shear rate (WSR) is an important stimulus for the brachial artery flow-mediated dilation (FMD) response. However, WSR estimation near the arterial wall by conventional Doppler is inherently difficult. To overcome this limitation, we utilised multi-gate Doppler to accurately determine the WSR stimulus near the vessel wall simultaneously with the FMD response using an integrated FMD system [Ultrasound Advanced Open Platform (ULA-OP)]. Using the system, we aimed to perform a detailed analysis of WSR-FMD response and establish novel WSR parameters in a healthy young population. Data from 33 young healthy individuals (27.5±4.9yrs, 19F) were analysed. FMD was assessed with reactive hyperemia using ULA-OP. All acquired raw data were post-processed using custom-designed software to obtain WSR and diameter parameters. The acquired velocity data revealed that non-parabolic flow-profiles within the cardiac cycle and under different flow-states, with heterogeneity between participants. We also identified seven WSR magnitude and four WSR time-course parameters. Among them, WSR area under the curve until its return to baseline was the strongest predictor of the absolute (R^2=0.25) and percentage (R^2=0.31) diameter changes in response to reactive hyperemia. For the first time, we identified mono- and biphasic WSR stimulus patterns within our cohort that produced different magnitudes of FMD response [absolute diameter change: 0.24±0.10mm (monophasic) vs 0.17±0.09mm (biphasic), p<0.05]. We concluded that accurate and detailed measurement of the WSR stimulus is important to comprehensively understand the FMD response and that this advance in current FMD technology could be important to better understand vascular physiology and pathology.

Key Words

Endothelial function; Reactive hyperemia; Ultrasound; Vasodilation; Wall shear stress.

New & Noteworthy

An estimation of wall shear rate (WSR) near the arterial wall by conventional Doppler ultrasound is inherently difficult. Using a recently-developed integrated FMD ultrasound system, we were able to accurately estimate WSR near the wall, and identified a number of novel WSR variables that may prove to be useful in the measurement of endothelial function, an important biomarker of vascular physiology and disease.

68 **INTRODUCTION:**

69 Brachial artery flow mediated dilation (FMD) has been used extensively to assess the
70 function and health of the vascular endothelium since its first use by Celermajer et al (5).
71 However, a persistent problem with this method is the inability to accurately measure the
72 wall shear stress *stimulus* that produces the measured FMD *response*. This is a perplexing
73 problem that has resulted in the extensive use of Doppler ultrasound peak velocity to
74 estimate wall shear stress, or its surrogate, wall shear rate (WSR). This is currently the only
75 practical solution available when measuring FMD, but this method underestimates WSR (22)
76 and is a blunt instrument to dissect the complex and dynamic WSR events occurring during
77 FMD.

78

79 In the absence of WSR data, the accurate interpretation of the FMD response may be
80 confounded and this has likely limited its full potential as a scientific and clinical tool. For
81 example, the mechanisms of diminished FMD could involve impaired brachial artery
82 endothelial function or alternatively could result from altered microvascular function
83 blunting the hyperaemic response and, in turn, WSR stimulus. Knowledge of the WSR
84 stimulus may also help to resolve and exploit issues relating to differences in baseline
85 diameter and 'low-flow' vasoconstriction occurring during cuff-occlusion (2, 11, 26),
86 providing a more comprehensive characterization of the underlying vascular physiology.

87

88 For physiological studies, the optimal tool for FMD needs to combine continuous and
89 simultaneous measurement of WSR and vessel diameter in order to comprehensively
90 characterise the WSR-FMD stimulus-response relationship. We have previously reported a
91 method to simultaneously measure WSR and vessel diameter during FMD (28). Unlike the

estimation of WSR from Doppler ultrasound, this system uses multi-gate spectral Doppler to acquire velocity data at different sites across the vessel diameter and close to the vessel wall, producing a continuous velocity profile from near to far wall (27). These data can be used to generate a detailed spectral Doppler profile across the vessel diameter and close to the vessel wall to accurately determine WSR (27). This overcomes the limitation of a single pulsed-wave Doppler sample-gate and the need to assume a perfect parabolic velocity profile (12).

Using this method we were able to show that estimation of WSR by conventional Doppler ultrasound is inaccurate (28), at least partly because the presumed parabolic velocity profile (15) is often asymmetric during hyperaemia and varies considerably through the cardiac cycle (12, 23, 28). Because of this, the extant literature presents a well characterised arterial diameter response to reactive hyperaemia, but lacks a well characterised WSR stimulus.

We have recently enhanced and refined this system in a collaborative effort between engineers, clinicians and physiologists with extensive experience of using ultrasound, to provide a sophisticated tool that can advance current FMD technology. This novel tool has an additional acquisition system capable of storing the large amount of raw data generated during the FMD procedure (18, 19). This has vastly expanded data collection capacity so that it can continuously measure WSR and vessel diameter over an extended period of time to provide accurate, detailed and simultaneous WSR-FMD stimulus-response data.

Here we report, for the first time, the use of this method. Our overall aim was to establish a new benchmark in WSR-FMD measurement. First, we wanted to establish the relevant

variables derived from the measurement system. Second, because the WSR-FMD response in humans is currently unknown, we wanted to establish a 'normal reference' by conducting a detailed analysis of the WSR-FMD response in a cohort of healthy young adults. Third, we wanted to determine which WSR variables were the best predictors of a normal FMD response. Fourth, we wanted to investigate the patterns of WSR during hyperaemia and determine whether these influenced the FMD response. We had noticed two distinct WSR patterns during our pilot work: A 'monophasic' pattern, where WSR increases sharply reaching its peak in one go during hyperaemia; and a 'biphasic' pattern, where WSR increases sharply followed by a slow increase before reaching its peak during hyperaemia. These two distinct WSR patterns cannot readily be seen with conventional Doppler and we wanted to know if the biphasic WSR pattern resulted in a greater magnitude of hyperaemic WSR than the monophasic WSR pattern, and if so, whether this greater WSR produced a greater brachial artery vasodilatory response than the monophasic WSR pattern.

METHODS:

Participants

Thirty-three young individuals (27.5±4.9 yrs, 19 females) participated in this study. Of these, 15 participants were studied in Exeter, UK and 18 in Pisa, Italy. All were healthy, without hypertension, type 2 diabetes, dyslipidaemia, or overt cardiovascular disease. UK National Research Ethics Service South West Committee and the institutional ethics committee at University of Pisa approved all study procedures and written informed consent was obtained from all participants.

Experimental procedures

Participants arrived in our temperature-controlled laboratories after an overnight fast, had blood samples drawn for biochemical analysis, consumed a standardized meal and rested for 20 min before initiation of the study protocol.

Brachial artery FMD was assessed non-invasively following established guidelines (6, 10, 24) and as previously described by us elsewhere (2, 8, 9). Briefly, participants lay supine on an examination bed with the right arm fixed in position and immobilised using a positioning pillow on a metal table. A small blood pressure cuff was placed around the proximal part of the forearm. A complete and open research system for ultrasound imaging and acquisition, the Ultrasound Advanced Open Platform (ULA-OP; Microelectronics Systems Design Laboratory, University of Florence, Italy) was connected to a high-frequency linear array transducer LA523 (Esaote SpA, Florence, Italy) and used to obtain both B-mode and multi-gate velocity data from the brachial artery (4). Once the optimal ultrasound image was obtained, the transducer was carefully clamped to prevent movement during the procedure using a custom-designed transducer holder. If necessary, a micro-adjuster was used to obtain a precisely aligned image.

Baseline brachial artery image and blood velocity were recorded for 60 s. Reactive hyperemia was then induced by rapidly inflating the forearm cuff (AI6, Hokanson, Bellevue, WA) to 250 mmHg to occlude forearm blood flow for 5 min. At 5 min, the cuff was rapidly deflated. Recording was restarted 30 s before deflation and continued until 5 min following deflation.

In a sub-set of participants (n=13), baseline brachial artery diameter measurements were repeated after a 15 min rest period, and endothelium-independent dilation was assessed using sub-lingual nitroglycerin spray (0.4 mg). A 60 s recording was started 9 min after administering the spray. We have previously found that measurement between 9 and 10 minutes after nitroglycerin administration captures maximal endothelial-independent vasodilation (unpublished observation).

Integrated FMD evaluation system

An integrated system capable of estimating both stimulus (WSR) and response (diameter) during the FMD assessment was developed by suitably modifying the existing hardware and software of the ULA-OP as well as by developing a post-processing software platform (19, 28). In particular, the ULA-OP offers much wider experimental possibilities than commercially-available Doppler ultrasound systems as it can be re-configured at run time and enables complete access to imaging data in every stage of the processing chain. The ULA-OP system also provides real-time imaging visualization functions in connection to a host personal computer. For the FMD data acquisition, an additional dedicated acquisition board was developed to store all raw (quadrature demodulated) echo data over a long time interval (up to 15 min). Furthermore, the ULA-OP system was recently upgraded to include the real-time measurement of arterial diameter (19).

In addition, a post-processing software platform was developed in order to evaluate endothelial function (19). It is based on Matlab® (The Mathwork Inc, Natick, MA) and consists of several processing blocks that, starting from the baseband acquired data, compute B-mode images and multi-gate spectral Doppler profiles. B-mode processing

187 organizes the data in lines and frames, interpolates them, applies 2D spatial filters, and
188 finally applies a logarithmic scale compression. Multi-gate spectral Doppler processing
189 reconstructs the information about the distribution of blood velocities at different depths
190 (256 up to 512 gates) through 256-point fast Fourier transforms (FFTs), hence the profiles
191 are low-pass filtered in order to remove the low-frequency spectral components through a
192 frequency domain mask. In cascade to the latter blocks, other specific processing blocks
193 extract wall positions of the artery and its diameter through a first order absolute central
194 moment (FOAM) algorithm (7), as well as WSR by a method that employs the direct
195 measurement of the whole velocity profile (20). Next, diameter and WSR time trends are
196 saved in output files which are finally loaded by a further Matlab® interface that extracts the
197 main parameters needed to investigate endothelial function.
198
199 ***Measurements of wall shear rate and diameter***
200 The signal elaboration system extracts detailed WSR parameters for describing both
201 magnitude and time-course of WSR changes. Seven WSR *magnitude* parameters were
202 analysed: 1) WSR at baseline, 2) WSR during low-flow, 3) WSR at peak hyperemia, 4)
203 absolute WSR increase from baseline, 5) percentage WSR increase from baseline, 6) area
204 under the WSR curve until time to peak dilation (WSR aucttp), and 7) area under the WSR
205 curve (WSR auc), measured between cuff release and the point at which WSR returned to
206 the baseline value. Four WSR *time-course* parameters were analysed: 1) first slope of WSR
207 increase during hyperemia (WSR SL1, an initial steep increase), 2) the second slope of WSR
208 increase during hyperemia (WSR SL2, a gradual increase after the initial steep increase; the
209 biphasic pattern only), 3) time to peak WSR (WSR Tp), and 4) time to return to baseline WSR
210 (WSR Tb). The monophasic and biphasic patterns of WSR increase were defined as: 1)

Monophasic - the peak WSR value was reached with a single, continuous steep increase only; 2) Biphasic - the peak WSR value was reached with an initial steep increase followed by a gradual second increase.

The signal elaboration system also extracts detailed diameter parameters. Three diameter *magnitude* parameters were analysed: 1) baseline diameter, 2) absolute diameter increase from baseline, and 3) percentage diameter increase from baseline. Two diameter *time-course* parameters were analysed: 1) time to peak diameter, and 2) time to return to baseline diameter, taken as the point at which diameter returns to its baseline values or plateaus.

Statistical analysis

Data are presented as means±SD for variables with a normal distribution, and median (interquartile range) for variables with a skewed distribution. A partial correlation analysis was performed between WSR parameters and diameter changes (absolute and percentage) controlling for the study centre in the whole cohort. A stepwise multivariate regression analysis was also performed in the whole cohort to determine the strongest predictor(s) of WSR parameters that were significantly associated with both absolute and percentage diameter changes in the partial correlation analysis (WSR at peak hyperaemia, WSR auc and absolute WSR increase from baseline). The study centre was also included as an independent variable in the model. Analysis of covariance (study centre as a covariate) was used to examine the differences in variables between monophasic and biphasic groups. A log-transformation was used for variables with skewed distribution before statistical

234 analysis. All statistical analysis was conducted using IBM SPSS Statistics 22 (IBM, Armonk,
235 NY). Significance was set at $p<0.05$.
236
237 **RESULTS:**
238 Selected baseline characteristics of the study participants are shown in Table 1. Body mass
239 index (24.1±3.0 vs 21.7±2.7 kg/m^2) and systolic blood pressure (121.5±7.5 vs 108.6±8.8
240 mmHg) were higher in male participants than female participants (both $p<0.05$). Other
241 participants' characteristics were similar between males and females.
242
243 ***Establishment of relevant WSR variables and their 'normal reference' values***
244 Figure 1 exhibits examples of multi-gate Doppler spectral profiles obtained at different time
245 points in the cardiac cycle at baseline and peak hyperemia, to illustrate the variability and
246 complexity of the WSR events occurring during FMD. A schematic description of detailed
247 WSR parameters extracted from the integrated FMD system is also presented in Figure 2. In
248 addition, parameters of WSR and diameter during brachial artery FMD and nitroglycerin-
249 mediated dilation in a healthy young cohort are shown in Table 2.
250
251 ***WSR variables that best predict a normal FMD response***
252 The results of partial correlation analysis between WSR parameters and diameter changes
253 during brachial artery FMD in the whole cohort are shown in Table 3. WSR at peak
254 hyperemia, WSR auc and absolute WSR increase were significantly associated with both
255 absolute and percentage diameter changes (all $p<0.05$). WSR SL1 and WSR aucttp were
256 significantly associated with percentage diameter changes (both $p<0.05$). We then
257 performed a stepwise multivariate regression analysis to determine the strongest WSR

predictor(s) of diameter changes during brachial artery FMD in the whole cohort. When WSR at peak hyperemia, WSR auc, absolute WSR increase and the study centre were all included in the same model at the same time, WSR auc was the best predictor of absolute brachial artery diameter change (β=0.503, R^2=0.25) and percentage diameter change (β=0.560, R^2=0.31). Collinearity statistics (tolerance and variance inflation factor) did not indicate a collinearity problem in this model. These associations remained significant when including WSR at baseline or baseline brachial artery diameter in the model above.

Influence of the WSR patterns during hyperemia on the FMD response

A schematic description of the monophasic and biphasic patterns of WSR increase is presented in Figure 3. Table 4 shows the parameters of WSR and diameter during brachial artery FMD and nitroglycerin-mediated dilation stratified by monophasic and biphasic WSR increase patterns. During reactive hyperemia, we observed the monophasic pattern of WSR increase in 15 participants (9 females) and the biphasic pattern of WSR increase in 18 participants (10 females). Individuals with the biphasic pattern showed a significantly greater WSR SL1 than those with the monophasic pattern (p<0.05). The parameters that were associated with diameter changes (WSR at peak hyperemia, WSR auc and absolute WSR increase from baseline) were significantly greater in the biphasic pattern than the monophasic pattern (Figure 4A-C). Similarly, individuals with the biphasic pattern showed a significantly greater WSR baseline and WSR aucttp than those with the monophasic pattern (all p<0.05). WSR Tp took longer in individuals with the biphasic pattern than in those with the monophasic pattern (p<0.05). The absolute diameter increase following reactive hyperemia was significantly greater in individuals with the biphasic pattern than in individuals with the monophasic pattern (0.24±0.10 mm vs 0.17±0.09 mm, p<0.05, Figure

5A). Percentage diameter increase tended to be greater in individuals with the biphasic pattern than individuals with the monophasic pattern (7.6±3.3 % vs 5.3±3.5 %, *p*=0.08, Figure 5B). However, to determine if WSR auc stimulus (the strongest predictor of FMD) explained the difference in FMD response between the two groups, we used an ANCOVA model that included WSR auc. This analysis showed that there were no differences in absolute or percentage brachial artery diameter change during FMD between the monophasic and biphasic groups when the WSR auc stimulus was taken into account (data not shown). Following nitroglycerin spray, there were no differences in WSR or change in brachial artery diameter between the mono- and biphasic groups (Table 4).

DISCUSSION:

Our main findings are that, using multi-gate spectral Doppler, we were able to acquire and extract seven WSR magnitude and four WSR time-course parameters over a long time-period to more comprehensively characterize the FMD response. We were also able to derive the first WSR-FMD stimulus-response data in humans using this method to provide a first point of reference in healthy, young adults. Furthermore, we were able to show that in this cohort, the WSR area under the curve until its return to baseline was the strongest predictor of the brachial artery diameter change in response to hyperemia. For the first time, we were able to identify mono- and biphasic WSR stimulus patterns within our cohort that produced different magnitude of FMD response. However, these responses were not different when the strongest WSR predictor (WSR auc) was statistically taken into account, illustrating the importance of knowing the WSR stimulus in order to correctly interpret the response.

Novel WSR variables, observations and comments on their values

We identified seven WSR magnitude variables and four WSR time-course variables that add novel measurements to the WSR-FMD response. These measurements took into account key phases of the FMD procedure and in combination with more traditional measurements, provide a comprehensive characterization of FMD-WSR response. Our data show that WSR is reduced during cuff-occlusion to about one-third that of baseline and that during reactive hyperaemia, peak WSR is almost six-times greater compared with baseline and is over 18-times greater compared with WSR during cuff-occlusion.

Our data also show that peak WSR was reached quickly (~12s) and preceded the time of peak dilation by an average of ~43s. We also note that the time taken to reach peak WSR was relatively homogenous between subjects, whereas there was considerable inter-individual variability in the time for diameter to reach peak diameter. The time taken for WSR to return to baseline (~104s) preceded the time for diameter to return to baseline in 15 participants but in the remaining 18, arterial diameter returned to baseline before WSR. The physiological mechanisms underlying this variability are unknown and were beyond the scope of this study, but putatively provide an opportunity to better understand the arterial response to the dynamic WSR changes during reactive hyperemia.

Multi-gate Doppler WSR auc is a good predictor of FMD

A key aim of the current study was to determine which WSR stimulus variable was the best predictor of the FMD response in healthy young adults. In a regression model that included the three WSR variables that were significantly associated with both absolute and relative diameter change (WSR peak, WSR auc and WSR absolute increase), we found that WSR auc

was the only predictor of both absolute (R^2=0.25) and relative (R^2=0.31) diameter changes, and this was the case irrespective of whether baseline diameter was included in the model. Given that WSR auc explains 25-31% of the variance in the regression model, it seems reasonable to conclude that this is an important predictor of the FMD response, whilst acknowledging the limitations of the R^2 statistics. Other factors influencing diameter change likely include the stiffness of the brachial artery, mechano-transduction of WSR to the endothelium, cell signalling in response to the transduced stimulus and the regulation of smooth muscle cell tone.

The association between WSR and the brachial artery FMD response has previously been reported in a cohort of young adults (14, 16, 17, 25). Using a similar cross-sectional study design as ours, Thijssen and colleagues found that WSR aucttp explained 14% of the variance in the FMD response in young healthy adults (25) and we found that WSR auc using our method explained 25-31% of the variance in the FMD response. This suggests that the WSR stimulus is an important contributor to the FMD response, but whether FMD should be 'normalized' to WSR is a contentious issue. Whereas some have suggested 'correcting (or normalizing)' data by dividing FMD by WSR (17), recent guidelines (24) recommend reporting WSR and FMD together without corrections. Consistent with this, where WSR has been measured with multi-gate Doppler, we suggest that the 'normal' stimulus-response characteristics should be reported as WSR auc and FMD together, and that the association between WSR auc and FMD are determined using statistical models. It was not the purpose of this study to determine this relationship in characteristically different populations or diseased populations; instead, the data presented here, together with the novel method of data acquisition, provide a platform for future studies of this nature.

Mono- and biphasic WSR responses in healthy young adults

An advantage of being able to continuously measure WSR was that we were able to observe, for the first time to our knowledge, two distinct patterns of WSR increase during reactive hyperemia: A 'monophasic' and a 'biphasic' WSR pattern that occurred between cuff release and peak WSR. Compared to the monophasic pattern, the biphasic pattern was associated with a greater magnitude as well as faster kinetics (steeper increase) of WSR increase during hyperemia. The biphasic pattern was also associated with a greater brachial artery vasodilatory response. However, when WSR auc stimulus was statistically taken into account, the vasodilatory response was no longer different between mono- and biphasic groups; that is, the dilation was matched to the WSR stimulus. This finding shows that within an otherwise characteristically similar cohort, there are two distinct vasodilatory responses to reactive hyperemia but that vasodilation is, ultimately, matched to the WSR stimulus.

The two different WSR responses may allude to underlying physiological differences between the cohorts, although their significance is unknown. It is possible that different mechanisms regulating blood flow during hyperemia produce the two different stimulus-response relationships. There are two candidate sites for the regulation of FMD: First, the arterial endothelium above the cuff that is experiencing an increase in WSR during hyperemia; second, the downstream microvasculature below the cuff that has dilated during cuff-occlusion and experiences a sudden increase in blood flow. During hyperemia, the endothelium of the brachial artery stimulates dilation in order to normalise the increased WSR brought about by hyperaemic flow. Differences in mechano-transduction of

WSR or differences in the paracrine response to the change in WSR could cause differences in the temporal pattern of WSR and magnitude of dilation. Microvascular function downstream of the cuff-occlusion site could also explain different WSR patterns (3, 13) because flow during reperfusion is influenced by downstream microvascular dilation (6). Microvessels also respond to reperfusion, including a vasoconstrictor response that likely influences upstream blood flow and, therefore, WSR. Consistent with this, we have previously shown distinct differences in the autoregulatory response to reperfusion by microvessels that temporally altered perfusion and oxygenation of tissue (1). Structural alterations in the microcirculation (21) can also influence its ability to respond to ischemia-reperfusion, which might influence the upstream WSR stimulus and explain differences between individuals. This is a first observation of two distinct WSR increase patterns and we did not explore control mechanisms in the first instance. Nor do we know if these WSR increase patterns are observed in characteristically different populations or diseased populations. Future studies will shed light on these issues and will ultimately determine whether there is value in determining two different WSR responses during the FMD assessment. But the ability to measure different hyperemic responses itself may be useful for future physiological studies.

The flow velocity profile is not always parabolic and symmetrical

One advantage of using multi-gate Doppler is that the flow velocity profile (normally assumed to be parabolic and symmetric, but which cannot be seen with conventional Doppler) can be seen in real time during data acquisition. One revelation from the current study was the heterogeneity in this flow-profile within the cardiac cycle, under different flow-states, and between subjects. During hyperemia, the shape of the parabola was seen

to be blunt, M-shaped, asymmetric and symmetric (see examples in Figure 1) and the shape of the parabola typically varied within the same cardiac cycle. Heterogeneity was also observed between subjects and was apparent at baseline, low-flow and during reactive hyperemia. These observations point to the importance of being able to detect flow velocity at different spatial points in the vessel in order to accurately measure WSR by extracting these local velocities.

'Low-flow' WSR and diameter during cuff-occlusion

We also found that all participants reduced WSR during cuff-occlusion but only 17 exhibited reduced brachial artery diameter (1 remained similar to baseline and 15 exhibited increased brachial artery diameter). This finding suggests that the brachial artery response to low-flow might be independent of WSR, at least in young, healthy adults.

Reduced vessel diameter immediately after cuff-release and its influence on WSR increase and diameter response

We noticed that immediately after cuff-release, 24 participants showed a reduced brachial artery diameter and nine did not. To determine whether this reduction of diameter immediately after cuff-release influenced the initial increase in WSR as well as the subsequent FMD response, we performed a sub-group analysis of participants stratified by the presence or absence of reduced brachial diameter. We found that absolute WSR increase (496.1±128.4 vs 477.6±134.4 1/s, p=0.733) and WSR SL1 (80.3±24.5 vs 78.7±25.5 $1/s^2$, p=0.874) were both similar between those with reduced brachial diameter and those without. Similarly, absolute diameter change (0.20±0.10 vs 0.22±0.12 mm, p=0.707) and relative diameter change (6.5±3.9 vs 6.8±3.9 %, p=0.852) were not different between those

426 with reduced diameter and those without. These observations indicate that the reduced
427 brachial artery diameter immediately after cuff-release does not play a major role in the
428 initial increase in WSR as well as the subsequent FMD response, at least in our population of
429 young, healthy adults. The reduction in diameter may be due to an acute pressure drop, a
430 brief period of turbulent flow, and alteration of smooth muscle cell tone or some
431 combination.
432
433 ***WSR response during nitroglycerin-mediated vasodilation***
434 There is a paucity of WSR data during the assessment of nitroglycerin-mediated
435 vasodilation. It has been used as an endothelium-independent control test to ensure the
436 validity of the FMD assessment. The application of nitroglycerin, thought to be an
437 exogenous nitric oxide donor, reduces smooth muscle cell tone and induces vasodilation. As
438 such, this has been considered WSR-independent and, thus, that there is no clear benefit for
439 acquiring WSR data during the assessment. Our observations support the position that
440 nitroglycerin-mediated vasodilation is WSR-independent, because WSR was slightly reduced
441 (Table 2) at the time that peak diameter occurred following administration of nitroglycerin.
442 Reduced WSR is likely a result of increased brachial artery diameter at the time of
443 measurement and suggests that nitroglycerin administration over-rides any effect of altered
444 WSR.
445
446 ***Implications from this study***
447 Our study highlights the importance of being able to measure the WSR stimulus as well as
448 the vasodilatory response to hyperemia. An accurate estimation of WSR close to the arterial
449 wall by conventional Doppler ultrasound, especially during reactive hyperemia, is inherently

difficult, further exacerbated by the uncertainties associated with the assumptions used to estimate WSR (especially that blood flow maintains a parabolic profile). We have shown that multi-gate Doppler overcomes these limitations by measuring blood flow velocity from near-to-far wall and by directly estimating WSR close to the arterial wall. By integrating these measurements with continuous and simultaneous measurement of arterial diameter, we were able to generate detailed information about the WSR stimulus and FMD response that has not been seen previously. For example, the system enabled us to reveal the monophasic and biphasic WSR patterns and allowed us to determine the most important WSR predictor of FMD. We are also able to characterise the 'normal WSR-FMD relationship in our cohort of healthy young adults, establishing a reference for these measurements. As such, we have demonstrated the usefulness of multi-gate Doppler as a modality for measuring arterial WSR, in this instance integrated into the ULA-OP system.

Overall, our study represents a technical advance that enables comprehensive WSR-FMD stimulus-response measurement within an integrated ultrasound system. The need to measure WSR continues to cause researchers to rely heavily on imprecise WSR data derived from vessel center-line peak velocity, creating uncertainties for the accurate interpretation of the FMD response. In a clinical setting, measurement of WSR has found little utility. Our broader aim is to provide a better tool for researchers and clinicians to augment the accuracy and usefulness of WSR-FMD measurement. This has the potential to expand current understanding of vascular physiology and pathophysiology, vascular ageing and the vascular response to interventions. In a clinical setting, this has the potential to improve clinical evaluation and management of patients with many diseases that involve blood vessels.

Limitations

We did not assess brachial artery stiffness which has been reported to affect the magnitude of FMD response (29) and may have contributed to the differences seen here. In addition, due to the cross-sectional nature of this study, we cannot infer any causation from our results. Finally, because multi-gate spectral Doppler is an extension of pulsed-wave (PW) Doppler, it has the same limitations of PW Doppler; for example, analysis limited to the axial velocity component (28) or possible velocity detection difficulties in the presence of high-level clutter.

CONCLUSION:

Overall, our results demonstrate the importance of being able to accurately determine a simultaneous WSR-FMD measurement, provide a reference for the 'normal' WSR-FMD response, and present a number of novel variables that may enable better understanding of vascular physiology and pathology.

ACKNOWLEDGEMENT:

We would like to thank the staff of the Diabetes and Vascular Medicine Research Centre, University of Exeter Medical School, for their valuable assistance to carry out this study.

GRANTS:

This study was supported by the European Union's Seventh Framework Programme (FP7/2007-2013) for the Innovative Medicine Initiative under grant agreement number IMI/115006 (the SUMMIT consortium), in part by the National Institute of Health Research

(NIHR) Exeter Clinical Research Facility, and by the Italian Ministry of University and Research (MIUR, Project PRIN 2010-2011). The views expressed are those of the authors and not necessarily those of the National Health Service, the NIHR, the Department of Health or the MIUR.

DISCLOSURE:

Nothing to disclose.

REFERENCES:

1. **Adingupu DD, Thorn CE, Casanova F, Elyas S, Gooding K, Gilchrist M, Aizawa K, Gates PE, Shore AC, and Strain DW**. Blood Oxygen Saturation After Ischemia is Altered With Abnormal Microvascular Reperfusion. *Microcirculation* 22: 294-305, 2015.
2. **Aizawa K, Elyas S, Adingupu DD, Casanova F, Gooding KM, Strain WD, Shore AC, and Gates PE**. Reactivity to low-flow as a potential determinant for brachial artery flow-mediated vasodilatation. *Physiological reports* 4: e12808, 2016.
3. **Anderson TJ, Charbonneau F, Title LM, Buithieu J, Rose MS, Conradson H, Hildebrand K, Fung M, Verma S, and Lonn EM**. Microvascular Function Predicts Cardiovascular Events in Primary Prevention: Long-Term Results From the Firefighters and Their Endothelium (FATE) Study. *Circulation* 123: 163-169, 2011.
4. **Boni E, Bassi L, Dallai A, Guidi F, Ramalli A, Ricci S, Housden J, and Tortoli P**. A reconfigurable and programmable FPGA-based system for nonstandard ultrasound methods. *IEEE Trans Ultrason Ferroelectr Freq Control* 59: 1378-1385, 2012.
5. **Celermajer DS, Sorensen KE, Gooch VM, Spiegelhalter DJ, Miller OI, Sullivan ID, Lloyd JK, and Deanfield JE**. Non-invasive detection of endothelial dysfunction in children and adults at risk of atherosclerosis. *Lancet* 340: 1111-1115, 1992.
6. **Corretti MC, Anderson TJ, Benjamin EJ, Celermajer D, Charbonneau F, Creager MA, Deanfield J, Drexler H, Gerhard-Herman M, Herrington D, Vallance P, Vita J, and Vogel R**. Guidelines for the ultrasound assessment of endothelial-dependent flow-mediated vasodilation of the brachial artery: a report of the International Brachial Artery Reactivity Task Force. *J Am Coll Cardiol* 39: 257-265, 2002.
7. **Demi M, Paterni M, and Benassi A**. The First Absolute Central Moment in Low-Level Image Processing. *Comput Vis Image Underst* 80: 57-87, 2000.
8. **Gates PE, Boucher ML, Silver AE, Monahan KD, and Seals DR**. Impaired flow-mediated dilation with age is not explained by L-arginine bioavailability or endothelial asymmetric dimethylarginine protein expression. *J Appl Physiol* 102: 63-71, 2007.
9. **Gilchrist M, Winyard PG, Aizawa K, Anning C, Shore A, and Benjamin N**. Effect of dietary nitrate on blood pressure, endothelial function, and insulin sensitivity in type 2 diabetes. *Free Radic Biol Med* 60: 89-97, 2013.
10. **Harris RA, Nishiyama SK, Wray DW, and Richardson RS**. Ultrasound assessment of flow-mediated dilation. *Hypertension* 55: 1075-1085, 2010.

11. **Irace C, Tripolino C, Scavelli FB, Carallo C, and Gnasso A**. Brachial Low-Flow-Mediated Constriction is Associated with Delayed Brachial Flow-Mediated Dilation. *J Atheroscler Thromb* 23: 355-363, 2016.
12. **Krams R, Bambi G, Guidi F, Helderman F, van der Steen AF, and Tortoli P**. Effect of vessel curvature on Doppler derived velocity profiles and fluid flow. *Ultrasound Med Biol* 31: 663-671, 2005.
13. **Mitchell GF, Parise H, Vita JA, Larson MG, Warner E, Keaney JF, Jr., Keyes MJ, Levy D, Vasan RS, and Benjamin EJ**. Local shear stress and brachial artery flow-mediated dilation: the Framingham Heart Study. *Hypertension* 44: 134-139, 2004.
14. **Padilla J, Johnson BD, Newcomer SC, Wilhite DP, Mickleborough TD, Fly AD, Mather KJ, and Wallace JP**. Adjusting flow-mediated dilation for shear stress stimulus allows demonstration of endothelial dysfunction in a population with moderate cardiovascular risk. *J Vasc Res* 46: 592-600, 2009.
15. **Papaioannou TG, Karatzis EN, Vavuranakis M, Lekakis JP, and Stefanadis C**. Assessment of vascular wall shear stress and implications for atherosclerotic disease. *Int J Cardiol* 113: 12-18, 2006.
16. **Pyke KE, Dwyer EM, and Tschakovsky ME**. Impact of controlling shear rate on flow-mediated dilation responses in the brachial artery of humans. *J Appl Physiol* 97: 499-508, 2004.
17. **Pyke KE, and Tschakovsky ME**. Peak vs. total reactive hyperemia: which determines the magnitude of flow-mediated dilation? *J Appl Physiol* 102: 1510-1519, 2007.
18. **Ramalli A, Bassi L, Lenge M, Palombo C, Aizawa K, and Tortoli P**. An Integrated System for the Evaluation of Flow Mediated Dilation. *Int Conf Acoust Spee* 5145–5148, 2014.
19. **Ramalli A, Byra M, Dallai A, Palombo C, Aizawa K, Sbragi S, Shore A, and Tortoli P**. A Multiparametric Approach Integrating Vessel Diameter, Wall Shear Rate and Physiologic Signals for Optimized Flow Mediated Dilation Studies. *Ieee Int Ultra Sym* 1-4, 2015.
20. **Ricci S, Swillens A, Ramalli A, Segers P, and Tortoli P**. Wall shear rate measurement: Validation of a new method through multi-physics simulations. *IEEE Trans Ultrason Ferroelectr Freq Control* 64: 66-77, 2017.
21. **Schiffrin EL**. Remodeling of resistance arteries in essential hypertension and effects of antihypertensive treatment. *Am J Hypertens* 17: 1192-1200, 2004.
22. **Silber HA, Ouyang P, Bluemke DA, Gupta SN, Foo TK, and Lima JA**. Why is flow-mediated dilation dependent on arterial size? Assessment of the shear stimulus using phase-contrast magnetic resonance imaging. *Am J Physiol Heart Circ Physiol* 288: H822-828, 2005.
23. **Stoner L, Sabatier ML, and Young JM**. Examination of possible flow turbulence during flow-mediated dilation testing. *Open J Med Imag* 1: 1-8, 2011.
24. **Thijssen DH, Black MA, Pyke KE, Padilla J, Atkinson G, Harris RA, Parker B, Widlansky ME, Tschakovsky ME, and Green DJ**. Assessment of flow-mediated dilation in humans: a methodological and physiological guideline. *Am J Physiol Heart Circ Physiol* 300: H2-12, 2011.
25. **Thijssen DH, Bullens LM, van Bemmel MM, Dawson EA, Hopkins N, Tinken TM, Black MA, Hopman MT, Cable NT, and Green DJ**. Does arterial shear explain the magnitude of flow-mediated dilation?: a comparison between young and older humans. *Am J Physiol Heart Circ Physiol* 296: H57-64, 2009.
26. **Thijssen DH, van Bemmel MM, Bullens LM, Dawson EA, Hopkins ND, Tinken TM, Black MA, Hopman MT, Cable NT, and Green DJ**. The impact of baseline diameter on flow-mediated dilation differs in young and older humans. *Am J Physiol Heart Circ Physiol* 295: H1594-1598, 2008.
27. **Tortoli P, Morganti T, Bambi G, Palombo C, and Ramnarine KV**. Noninvasive simultaneous assessment of wall shear rate and wall distension in carotid arteries. *Ultrasound Med Biol* 32: 1661-1670, 2006.
28. **Tortoli P, Palombo C, Ghiadoni L, Bini G, and Francalanci L**. Simultaneous ultrasound assessment of brachial artery shear stimulus and flow-mediated dilation during reactive hyperemia. *Ultrasound Med Biol* 37: 1561-1570, 2011.

588 29. **Witte DR, van der Graaf Y, Grobbee DE, and Bots ML**. Measurement of flow-mediated
589 dilatation of the brachial artery is affected by local elastic vessel wall properties in high-risk patients.
590 *Atherosclerosis* 182: 323-330, 2005.

591 **FIGURE LEGENDS:**

592 **Figure 1.** Examples of multi-gate spectral Doppler profiles obtained from the ULA-OP
593 system, in red-to-white color scale, and the related mean frequency, which is overlaid in
594 blue. The first row shows multi-gate spectral Doppler profiles at baseline at different time
595 points in the cardiac cycle from the same individual (1A, early systole; 1B, peak systole; 1C,
596 early diastole). The second row shows multi-gate spectral Doppler profiles during peak
597 hyperemia at the same time points in the cardiac cycle as Fig 1A-C from the same
598 participant (1D, early systole; 1E, peak systole; 1F, early diastole). The third row shows
599 multi-gate spectral Doppler profiles during peak hyperemia at the same time points as Fig
600 1D-F in the cardiac cycle but from a different participant (1G, early systole; 1H, peak systole;
601 1J, early diastole). Note the asymmetry in velocity in some profiles (e.g. 1E, 1H and 1J), blunt
602 profile (1F) and M-shaped profile (1G). Also note the differences in spectral profile during
603 cardiac cycle as well as between participants. Sub 1, subject 1; Sub 2, subject 2.

604

605 **Figure 2.** A schematic description of WSR parameters obtained from brachial artery FMD
606 assessment using continuous multi-gate Doppler and simultaneous diameter. In the upper
607 panel, traces in light blue and red represent the peak and mean values of WSR, respectively.
608 In the lower panel, traces in light blue and red represent the variations in diameter (due to
609 cardiac cycle) and mean diameter of the brachial artery, respectively. WSR, wall shear rate;
610 SL1, first slope of wall shear rate increase; SL2, second slope of wall shear rate increase;
611 aucttp, area under the curve until time to peak dilation (area shaded with turquoise); auc,
612 area under the curve until its return to baseline level (area shaded both with turquoise and
613 grey); Tp, time to peak value; Tb, time to return to baseline value; Δ, changes.

614

615 **Figure 3.** Representative examples of monophasic (upper panel) and biphasic (lower panel)
616 patterns of WSR increase and diameter changes during brachial artery FMD assessment.
617 Traces in red represent a mean value of WSR or brachial artery diameter.
618
619 **Figure 4.** WSR at peak hyperemia (A), WSR auc (B) and absolute WSR increase from baseline
620 (C) between monophasic (n=15) and biphasic (n=18) WSR increase patterns. Data are shown
621 as means±SE. *Significantly different from the monophasic group (p<0.05).
622
623 **Figure 5.** Absolute diameter changes (A) and percentage diameter changes (B) between
624 monophasic (n=15) and biphasic (n=18) WSR increase patterns. Data are shown as
625 means±SE. *Significantly different from the monophasic group (p<0.05).

626 **Table 1. Selected characteristics of the study participants**

627

	Values
Participants, n	33
Age, yrs	27.5±4.9
Sex, m/f	14/19
BMI, kg/m^2	22.7±3.1
Systolic BP, mmHg	114.1±10.4
Diastolic BP, mmHg	69.2±6.6
Heart Rate, bpm	64.2±9.5

628

629 Data are means±SD or numbers. BMI, body mass index; BP, blood pressure.

Table 2. Parameters of wall shear rate and diameter during brachial artery flow-mediated dilation and nitroglycerin-mediated dilation assessments in a healthy young cohort

	Values	Ranges
Flow-mediated dilation (n=33)		
WSR magnitude parameters		
WSR baseline, 1/s	103.9±54.9	17.5 - 222.6
WSR low-flow, 1/s	32.6±23.4	-1.8 - 94.9
WSR peak, 1/s	594.9±158.2	269.1 - 924.6
WSR Δ, 1/s	491.0±160.7	188.4 - 845.0
WSR %Δ, %	564 (267-994)	155.2 - 3270.5
WSR aucttp, au	13414±5629	3515 - 30540
WSR auc, au	17337±6724	4064 - 39473
WSR time-course parameters		
WSR SL1, $1/s^2$	79.9±27.3	24.3 - 126.3
WSR SL2, $1/s^2$*	16.4±8.8	0.33 - 35.4
WSR Tp, s	12.2±2.6	7.3 - 20.6
WSR Tb, s	104.1±36.6	57.5 - 182.5
Diameter magnitude parameters		
Diameter baseline, mm	3.29±0.45	2.57 - 4.24
Diameter Δ, mm	0.21±0.10	0.03 - 0.47
Diameter %Δ, %	6.5±3.5	0.95 - 14.8
Diameter time-course parameters		
Diameter Tp, s	55.3±31.2	26.8 - 197.9
Diameter Tb, s	113.6±59.8	10.5 - 249.5
Nitroglycerin-mediated dilation (n=13)		
WSR magnitude parameters		
WSR baseline, 1/s	58.6±20.9	33.1 - 101.2
WSR peak dilation, 1/s	44.7±24.6	17.9 - 87.8
Diameter magnitude parameters		
Baseline diameter, mm	3.51±0.56	2.48 - 4.30
Diameter Δ, mm	0.77±0.15	0.56 - 1.10
Diameter %Δ, %	22.5±4.8	13.8 - 28.4

Data are means±SD for variables with normal distribution, median (interquartile range) for variables with skewed distribution, and range of each variable (minimum to maximum). *Obtained from 18 participants who showed the biphasic WSR increase response. WSR, wall shear rate; SL1, first slope of wall shear rate increase; SL2, second slope of wall shear rate increase; aucttp, area under the curve until time to peak dilation; auc, area under the curve until its return to baseline value; Tp, time to peak value; Tb, time to return to baseline value; Δ, changes.

Table 3. Partial correlation analysis between parameters of WSR and diameter changes in the whole cohort.

	Diameter Δ	Diameter % Δ
WSR baseline	*r*=0.18, *p*=0.327	*r*=0.13, *p*=0.470
WSR low-flow	*r*=0.32, *p*=0.072	*r*=0.32, *p*=0.077
WSR SL1	*r*=0.35, *p*=0.053	*r*=0.36, *p*=0.041
WSR SL2*	*r*=0.17, *p*=0.524	*r*=0.24, *p*=0.353
WSR peak	*r*=0.41, *p*=0.020	*r*=0.47, *p*=0.007
WSR Δ	*r*=0.41, *p*=0.021	*r*=0.49. *p*=0.004
WSR %Δ	*r*=0.04, *p*=0.843	*r*=0.11, *p*=0.558
WSR aucttp	*r*=0.34, *p*=0.061	*r*=0.42, *p*=0.017
WSR auc	*r*=0.46, *p*=0.008	*r*=0.56, *p*=0.001
WSR Tp	*r*=0.32, *p*=0.072	*r*=0.32, *p*=0.079
WSR Tb	*r*=0.04, *p*=0.109	*r*=0.35, *p*=0.052

*Obtained from 18 participants who showed the biphasic WSR increase response. WSR, wall shear rate; SL1, first slope of wall shear rate increase; SL2, second slope of wall shear rate increase; aucttp, area under the curve until time to peak dilation; auc, area under the curve until its return to baseline value; Tp, time to peak value; Tb, time to return to baseline value; Δ, changes.

Table 4. Parameters of wall shear rate and diameter during brachial artery flow-mediated dilation and nitroglycerin-mediated dilation assessments stratified by monophasic and biphasic patterns of wall shear rate increase.

	Monophasic (n=15)	Biphasic (n=18)
Flow-mediated dilation		
WSR magnitude parameters		
WSR baseline, 1/s	89.6±54.6	115.9±53.8*
WSR low-flow, 1/s	32.7±23.8	32.5±23.7
WSR %Δ, %	596(181-1374)	552(286-735)
WSR aucttp, au	10784±4961	15607±5309*
WSR time-course parameters		
WSR SL1, $1/s^2$	68.8±30.0	89.1±21.5*
WSR SL2, $1/s^2$	-	16.4±8.8
WSR Tp, s	11.1±3.2	13.2±1.6*
WSR Tb, s	92.1±31.9	114.1±38.1
Diameter magnitude parameters		
Diameter baseline, mm	3.29±0.44	3.28±0.47
Diameter time-course parameters		
Diameter Tp, s	56.6±43.8	54.2±15.8
Diameter Tb, s	110.8±62.3	116.0±59.3
Nitroglycerin-mediated dilation (5 monophasic and 8 biphasic)		
WSR magnitude parameters		
WSR baseline, 1/s	43.0±10.2	68.4±20.1*
WSR peak dilation, 1/s	38.9±21.5	48.3±27.0
Diameter magnitude parameters		
Baseline diameter, mm	3.38±0.60	3.59±0.56
Diameter Δ, mm	0.83±0.10	0.74±0.17
Diameter %Δ, %	25.0±3.9	21.0±4.8

Data are means±SD for variables with normal distribution, and median (interquartile range) for variables with skewed distribution. *significantly different from the monophasic group (p<0.05). WSR, wall shear rate; SL1, first slope of wall shear rate increase; SL2, second slope of wall shear rate increase; aucttp, area under the curve until time to peak dilation; auc, area under the curve until its return to baseline value; Tp, time to peak value; Tb, time to return to baseline value; Δ, changes.

Figure 1.

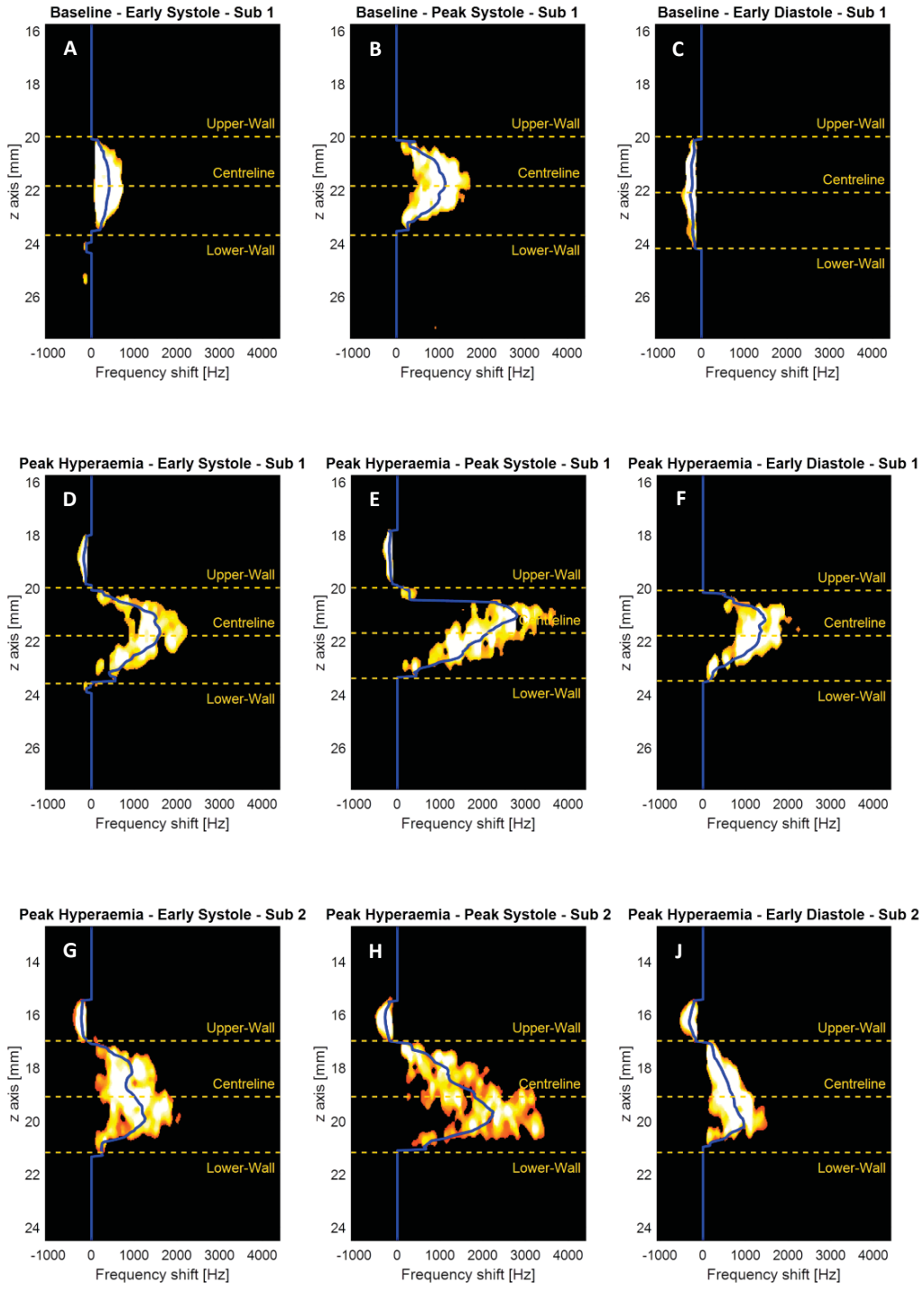
Baseline - Early Systole - Sub 1
Baseline - Peak Systole - Sub 1
Baseline - Early Diastole - Sub 1
Peak Hyperaemia - Early Systole - Sub 1
Peak Hyperaemia - Peak Systole - Sub 1
Peak Hyperaemia - Early Diastole - Sub 1
Peak Hyperaemia - Early Systole - Sub 2
Peak Hyperaemia - Peak Systole - Sub 2
Peak Hyperaemia - Early Diastole - Sub 2
A
B
C
D
E
F
G
H
J
Upper-Wall
Centreline
Lower-Wall
z axis [mm]
Frequency shift [Hz]

Figure 2.

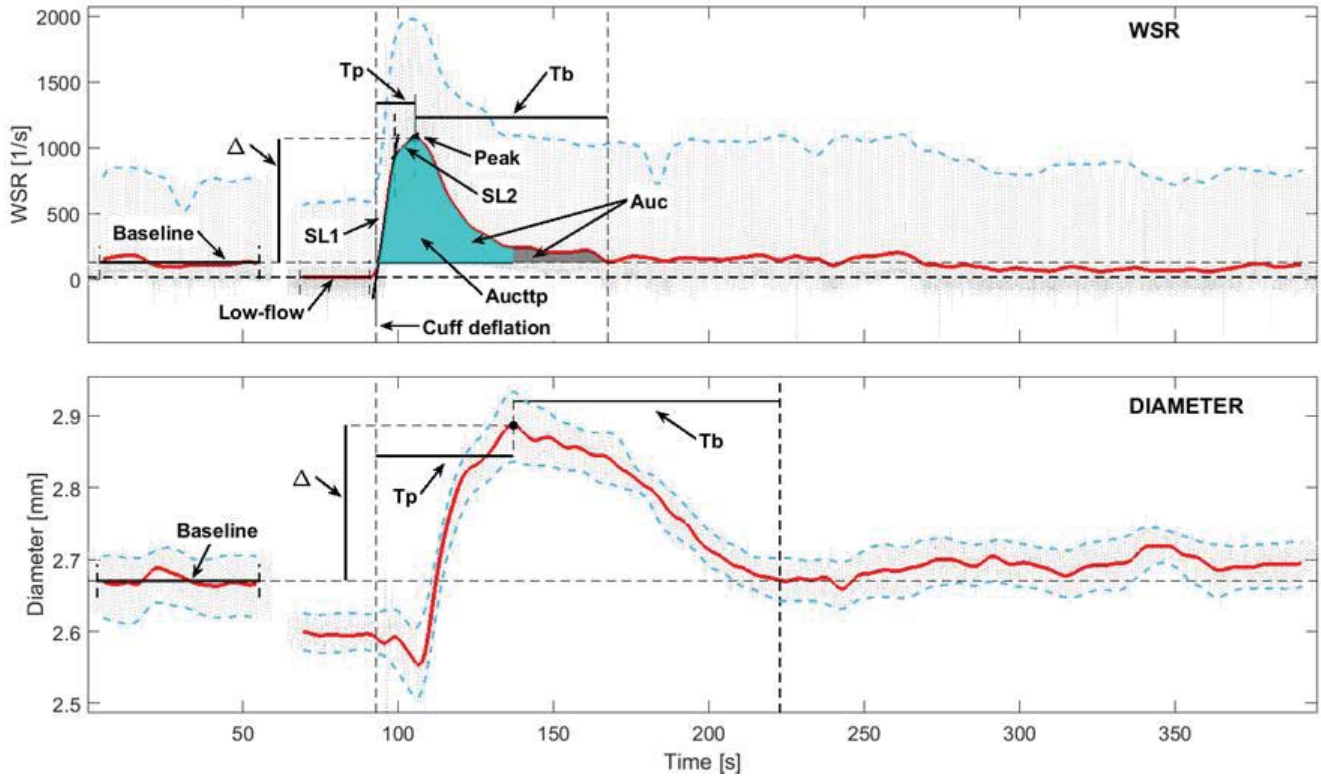
WSR
WSR [1/s]
2000
1500
1000
500
0
Tp
Tb
Δ
Peak
SL2
Auc
Baseline
SL1
Aucttp
Low-flow
Cuff deflation
DIAMETER
Diameter [mm]
2.9
2.8
2.7
2.6
2.5
Tb
Δ
Tp
Baseline
50
100
150
200
250
300
350
Time [s]

Figure 3.

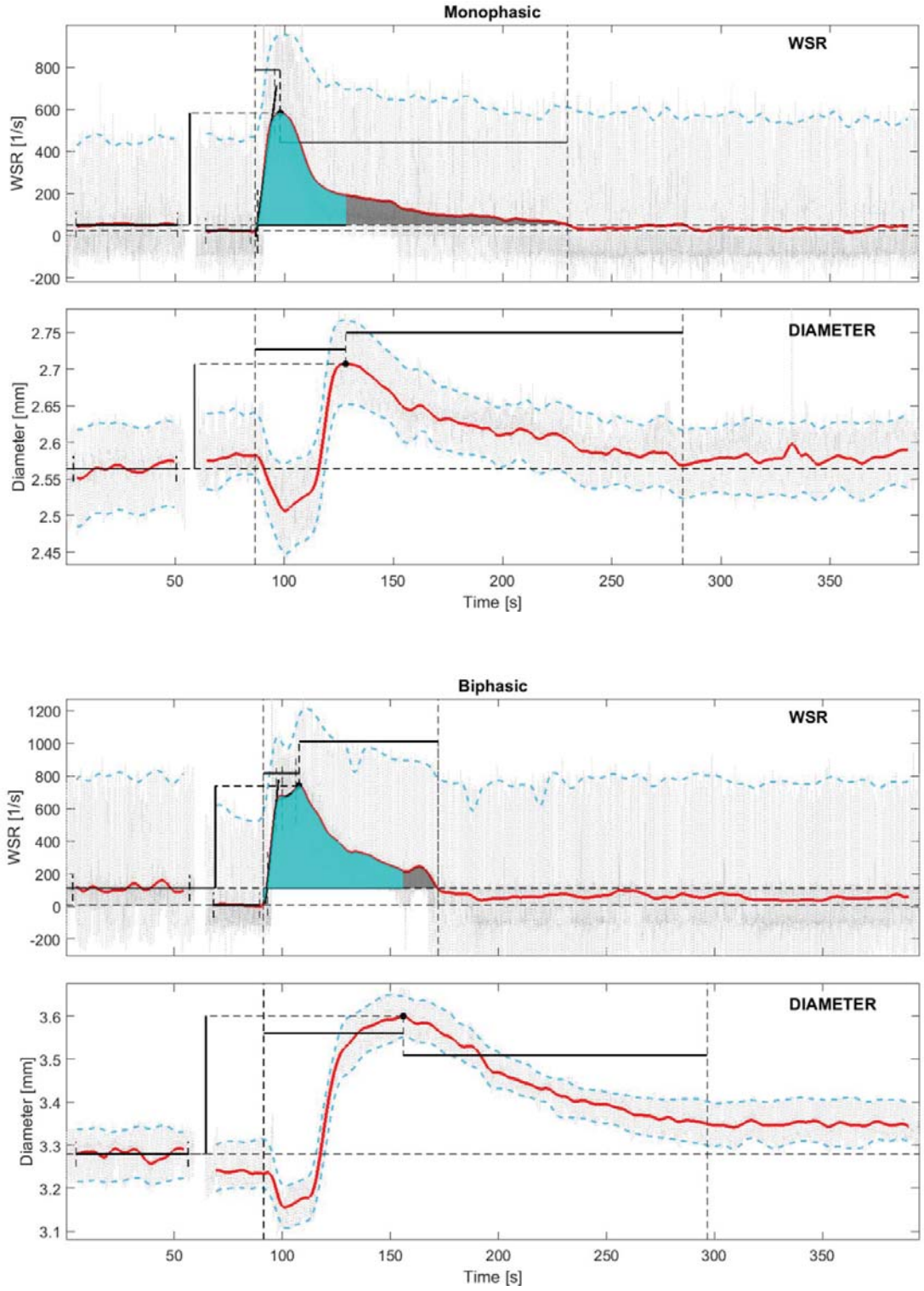
Monophasic
WSR
WSR [1/s]
800
600
400
200
0
-200
DIAMETER
Diameter [mm]
2.75
2.7
2.65
2.6
2.55
2.5
2.45
50
100
150
200
250
300
350
Time [s]
Biphasic
WSR
WSR [1/s]
1200
1000
800
600
400
200
0
-200
DIAMETER
Diameter [mm]
3.6
3.5
3.4
3.3
3.2
3.1
50
100
150
200
250
300
350
Time [s]

Figure 4.

A

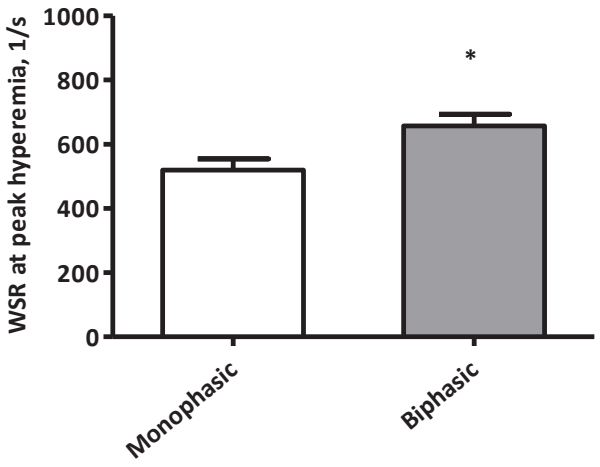
WSR at peak hyperemia, 1/s
1000
800
600
400
200
0
*
Monophasic
Biphasic

B

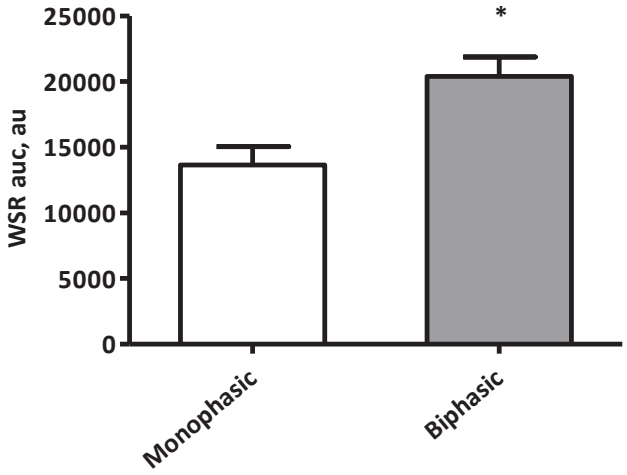
WSR auc, au
25000
20000
15000
10000
5000
0
*
Monophasic
Biphasic

C

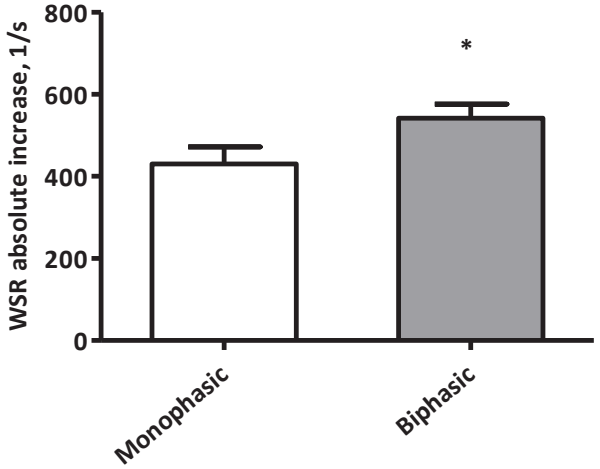
WSR absolute increase, 1/s
800
600
400
200
0
*
Monophasic
Biphasic

Figure 5.

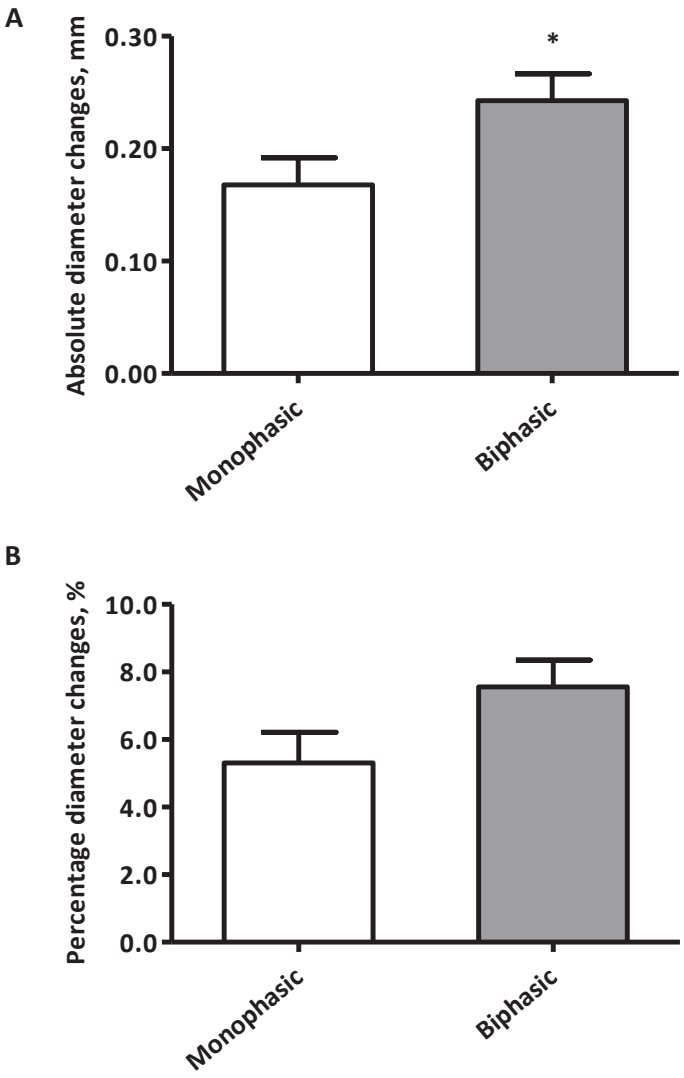
A
Absolute diameter changes, mm
0.30
0.20
0.10
0.00
*
Monophasic
Biphasic
B
Percentage diameter changes, %
10.0
8.0
6.0
4.0
2.0
0.0
Monophasic
Biphasic